Applied Microbiology and Biotechnology (2020) 104:9759–9771
https://doi.org/10.1007/s00253-020-10898-0

APPLIED MICROBIAL AND CELL PHYSIOLOGY

Deletion of the *pps*-like gene activates the cryptic *phaC* genes in *Haloferax mediterranei*

Junyu Chen[1,2] · Ruchira Mitra[1,3] · Hua Xiang[1,2] · Jing Han[1,2]

Received: 3 August 2020 / Revised: 1 September 2020 / Accepted: 7 September 2020 / Published online: 12 September 2020

Abstract

Haloferax mediterranei, a poly(3-hydroxybutyrate-*co*-3-hydroxyvalerate) (PHBV) producing haloarchaeon, possesses four PHA synthase encoding genes, *phaC*, *phaC1*, *phaC2*, and *phaC3*. In the wild-type strain, except *phaC*, the other three genes are cryptic and not transcribed under PHA-accumulating conditions. The PhaC protein together with PhaE subunit forms the active PHA synthase and catalyzes PHBV polymerization. Previously, it was observed that the deletion of a gene named *pps*-like significantly enhanced PHBV accumulation probably resulted from the upregulation of *pha* cluster genes (*phaR-phaP-phaE-phaC*). The present study demonstrated the influence of *pps*-like gene deletion on the cryptic *phaC* genes. As revealed by qRT-PCR, the expression level of the three cryptic genes was upregulated in the ΔEPSΔ*pps*-like geneΔ*phaC* mutant. Sequential knockout of the cryptic *phaC* genes and fermentation experiments showed that PhaC1 followed by PhaC3 had the ability to synthesize PHBV in ΔEPSΔ*pps*-like geneΔ*phaC* mutant. Both PhaC1 and PhaC3 could complex with PhaE to form functionally active PHA synthase. However, the expression of *phaC2* did not lead to PHBV synthesis. Moreover, PhaC, PhaC1, and PhaC3 exhibited distinct substrate specificity as the 3HV content in PHBV copolymers was different. The EMSA result showed that PPS-like protein might be a negative regulator of *phaC1* gene by binding to its promoter region. Taken together, PhaC1 had the most pronounced effect on PHBV synthesis in ΔEPSΔ*pps*-like geneΔ*phaC* mutant and deletion of *pps*-like gene released the negative effect from *phaC1* expression and thereby restored PHBV accumulating ability in Δ*phaC* mutant.

Key points

- *Cryptic phaC genes were activated by pps-like gene deletion.*
- *PPS-like protein probably regulated phaC1 expression by binding to its promoter.*
- *Both PhaC1 and PhaC3 formed active PHA synthase with PhaE.*

Keywords *Haloferax mediterranei* · *pps*-like gene · Poly(3-hydroxybutyrate-*co*-3-hydroxyvalerate) · Cryptic *phaC* genes

Introduction

Nature has diverse ecosystem encompassing soda lakes, hot springs, deep oceans, deep sea hydrothermal vents, deserts, polar regions, etc. that exhibit extremities in one or more physico-chemical parameters. Microbiota inhabiting such environments includes varieties of extremophiles, such as halophiles, acidophiles, alkaliphiles, thermophiles, psychrophiles, piezophiles, xerotolerant, and radiotolerant (Orellana et al. 2018). Haloarchaea are the salt loving extremophiles belonging to *Archaea* domain. They are predominantly distributed in hypersaline environments such as soda lakes, natural brines, the Dead Sea, solar salterns, and rock salts (Fendrihan et al. 2006). Haloarchaea as an important microbial resource

✉ Hua Xiang
xiangh@im.ac.cn

✉ Jing Han
hanjing@im.ac.cn

[1] State Key Laboratory of Microbial Resources, Institute of Microbiology, Chinese Academy of Sciences, Beijing 100101, People's Republic of China

[2] College of Life Science, University of Chinese Academy of Sciences, Beijing 100049, People's Republic of China

[3] International College, University of Chinese Academy of Sciences, Beijing 100049, People's Republic of China

presents several advantages from an industrial point of view. For example, haloarchaeal enzymes are potential candidates for industrial applications under harsh conditions, where normal enzymes tend to be inactive or degrade. This is because haloarchaeal proteins are most likely to be salt-tolerant due to their adaptation to high salinity, resulting in high acidic amino acid content (Siroosi et al. 2014). Most haloarchaea are red and orange pigmented due to their ability to synthesize carotenoids (Zuo et al. 2018). Most importantly, haloarchaea are considered one of the most promising producers of polyhydroxyalkanoates (PHA) (Bhattacharyya et al. 2015). Until now, almost 17 haloarchaeal genera are known to produce PHA, including *Halopiger*, *Natrialba*, *Halobiforma*, *Haloarcula*, *Haloferax*, *Halococcus*, *Halogranum*, *Halorubrum*, *Natrinema*, and *Natronorubrum* (Hezayen et al. 2002; Legat et al. 2010; Zhao et al. 2015; Mitra et al. 2020).

PHA is a family of biodegradable and biocompatible polyester of hydroxyalkanoates synthesized by microbes as intracellular carbon and energy reserves under unbalanced conditions of nutrient limitation with excess carbon source (Han et al. 2007). Because of its good thermoplastic and mechanical properties, PHA is considered a potential alternative to the petroleum-based synthetic plastics. The characteristic properties of PHA are dependent on their monomer composition. For instance, poly(3-hydroxybutyrate) (PHB), the homopolymer of 3-hydroxybutyrate (3HB), is stiff and brittle in nature. It exhibits high degree of crystallization, early thermal degradation, and poor mechanical properties (Hong et al. 2013). Incorporation of 3-hydroxyvalerate (3HV) monomer in the PHB chain enhances their flexibility and mechanical properties (Han et al. 2015). Until now, more than 150 different types of monomers have been identified in PHA. Extensive research work has showed that PHA holds high promise as a biomaterial for developing medical implants for tissue engineering and wound healing (Han et al. 2017; Xue et al. 2018). Halophilic production of PHA is advantageous over non-halophiles because halophiles require less stringent sterile conditions as high salt concentrations prevent microbial contamination (Zhao et al. 2013). Moreover, haloarchaeal cells undergo lysis simply in tap water due to their high intracellular osmotic pressure (Shih et al. 2015). This eases the downstream processing. As a result, these factors contribute to reducing the overall PHA production cost.

Haloferax mediterranei is a model haloarchaea for studying archaeal physiology and metabolism. This strain accumulates poly(3-hydroxybutyrate-*co*-3-hydroxyvalerate) (PHBV) from various cheap unrelated carbon sources without using 3HV precursors (Hou et al. 2014). It efficiently utilizes several agro-industrial wastes, including vinasse, cheese whey, olive mill wastewater, and rice-based ethanol stillage, as low-cost substrates for PHBV production (Alsafadi and Al-Mashaqbeh 2017; Bhattacharyya et al. 2012; Bhattacharyya et al. 2014; Pais et al. 2016). Thus, it is the most prominent natural PHA producer among haloarchaea. The complete genome sequence of *H. mediterranei* was published in 2012 (Han et al. 2012). Subsequently, the key genes involved in PHBV metabolism and regulation have been identified and characterized in our lab (Cai et al. 2012; Cai et al. 2015; Han et al. 2013; Hou et al. 2013; Liu et al. 2015; Liu et al. 2016; Lu et al. 2008). The active PHA synthase in *H. mediterranei* is constituted of two subunits, PhaC and PhaE (Lu et al. 2008). Additionally, its genome sequence revealed three cryptic *phaC* genes, *phaC1*, *phaC2*, and *phaC3* (Han et al. 2010). Except *phaC2*, *phaC1* and *phaC3* encoded functional proteins which formed active PHA synthases with PhaE subunit and led to the synthesis of PHBV in *Haloarcula hispanica* PHB-1 (PHA synthase gene deletion mutant). These findings have further paved the way for developing engineered *H. mediterranei* strain. For example, the knockout mutant of exopolysaccharide (EPS) biosynthesis gene cluster, ΔEPS, showed a 20% higher PHBV production than the wild-type stain (Zhao et al. 2013). EPS is synthesized by the wild-type *H. mediterranei* and excreted into the medium. Its accumulation hinders PHA synthesis by enhancing the culture viscosity and consuming carbon source. The culture of ΔEPS exhibited a reduced viscosity and thus increased the dissolved oxygen content in the medium and decreased the foaming propensity. Furthermore, more carbon source was channeled towards PHBV synthesis in ΔEPS compared with the wild-type strain (Zhao et al. 2013).

In our recent research, we serendipitously discovered two mutants *H. mediterranei* ΔEPSΔ*pps* and ΔEPSΔ*pps*-like gene with further improved PHBV accumulation ability while characterizing the key enzymes involved in the interconversion of pyruvate and phosphoenolpyruvate (PEP) (Chen et al. 2019). PEP synthetase (PPS) catalyzed pyruvate to PEP. Its deletion strain ΔEPSΔ*pps* led to a 35.9% increase in PHA production which might be resulted from channeling more pyruvate to PHA synthesis. Notably, a novel protein that showed high homology with PPS, named PPS-like, was identified. However, unlike PPS, PPS-like protein did not participate in the conversion from pyruvate to PEP. Unexpectedly, its deletion increased PHBV production by 70.46%. Our RNA-seq data showed that several genes involved in the PHBV monomer supplying pathway (*bktB*, *phaB1*, *phaB2*, and *phaJ*) and PHBV biosynthesis (*phaR*, *phaP*, *phaE*, and *phaC*) were upregulated in ΔEPSΔ*pps*-like gene. This finding is speculated to result in a significantly increased PHBV accumulation. However, the definite mechanism behind the enhanced PHBV production remained to be determined.

The present paper is a continuation of our previous research work and attempts to determine the impact of *pps*-like gene deletion on the cryptic PHA synthase genes of *H. mediterranei* (Chen et al. 2019). We designed and

developed several PHA synthase mutant strains based on *H. mediterranei* ΔEPS Δ*pps*-like gene and checked its corresponding effects on PHBV synthesis. Overall, this study is an endeavor to elucidate the reasons behind improved PHBV synthesis upon *pps*-like gene deletion in *H. mediterranei*.

Materials and methods

Strains and growth conditions

All the bacterial and haloarchaeal strains used in this study are summarized in Table 1. The two *Escherichia coli* strains, JM109 and JM110, were used for constructing plasmids and eliminating DNA methylation of plasmids, respectively. They were grown in Luria-Bertani medium at 37 °C. When needed, 100 μg/mL ampicillin was added to the medium. *H. mediterranei* CGMCC 1.2087 (wild type strain) was deposited in the China General Microbiological Culture Collection Center (CGMCC). The derived strains of *H. mediterranei* used in this study were *pyrF* deletion mutants, and thus 50-μg/mL uracil was added to their culture media. They were cultivated in AS-168 medium (Sambrook et al. 1989) at 37 °C and used as seed cultures after entering late exponential phase. The seed culture was then inoculated into PHA production medium (Zhao et al. 2013) containing 10 g/L glucose with a 5% (vol/vol) inoculum for PHA synthesis. The fermentation was carried out at 37 °C until the glucose in the media was completely consumed.

Plasmid construction and genetic manipulation of *H. mediterranei*

The plasmids and primers used for gene knockout are listed in Table 1 and Table 2, respectively. The upstream and downstream fragments of the three *phaC* genes were amplified by using relevant primer pairs NF/NR and CF/CR from the genomic DNA of *H. mediterranei* via PCR, respectively. The three knockout plasmids, pHFX-*phaC*, pHFX-*phaC1*, and pHFX-*phaC3*, were constructed by inserting the two fragments of the target gene into the suicide plasmid pHFX (Liu et al. 2011). The plasmids were first constructed in *E. coli* JM109 and were confirmed by sequencing. Then, the plasmids extracted from *E. coli* JM110 were transformed into *H. mediterranei* by the polyethylene glycol-mediated method (Cline et al. 1989). The correct gene knockout mutants were screened by PCR verification as previously described (Liu et al. 2011).

RNA isolation and qRT-PCR

H. mediterranei cells were grown in PHA production medium in tubes to exponential phase and stationary phase and were subsequently harvested for RNA isolation. Total RNA extraction was carried out with the TRIzol® Reagent (Invitrogen, USA) as instructed by the manufacturer. cDNA was generated from the DNA-free RNA samples by using random hexamers and the MLV Reverse Transcriptase (Promega, USA). The fluorogenic quantitative PCR was performed in a ViiA™ 7 Real-Time PCR System (Applied Biosystems, USA) as described previously (Chen et al. 2019). Each sample was replicated in triplicates and normalized using 7S rRNA gene as an

Table 1 Strains and plasmids used in this study

Strains or plasmids	Relevant characteristics	Source and reference
Escherichia coli JM109	*recA1 supE44 endA1 hsdR17 gyrA96 relA1 thi*	(Sambrook et al. 1989)
E. coli JM110	*dam dcm* mutant of *E. coli* JM109	Novagen
H. mediterranei ΔEPS	EPS gene cluster deletion mutant of *H. mediterranei* DF50	(Zhao et al. 2013)
H. mediterranei ΔEPSΔ*pps*-like gene	*pps*-like gene deletion mutant of *H. mediterranei* ΔEPS	(Chen et al. 2019)
H. mediterranei ΔEPSΔ*pps*-like gene*ΔphaC*	*phaC* deletion mutant of *H. mediterranei* ΔEPSΔ*pps*-like gene	This study
H. mediterranei ΔEPSΔ*pps*-like gene*ΔphaCΔphaC1*	*phaC* and *phaC1* deletion mutant of *H. mediterranei* ΔEPSΔ*pps*-like gene	This study
H. mediterranei ΔEPSΔ*pps*-like gene*ΔphaCΔphaC3*	*phaC and phaC3* deletion mutant of *H. mediterranei* ΔEPSΔ*pps*-like gene	This study
H. mediterranei ΔEPSΔ*pps*-like gene*ΔphaCΔphaC1ΔphaC3*	*phaC*, *phaC1*, and *phaC3* deletion mutant of *H. mediterranei* ΔEPSΔ*pps*-like gene	This study
pHFX	4.0-kb integration vector, containing *pyrF* and its native promoter, Amp^r	(Liu et al. 2011)
pHFX-*phaC*	5.2 kb; integration vector of pHFX for *phaC* deletion	This study
pHFX-*phaC1*	5.2 kb; integration vector of pHFX for *phaC1* deletion	This study
pHFX-*phaC3*	5.2 kb; integration vector of pHFX for *phaC3* deletion	This study

Table 2 Primers used in this study

Primers	Sequence (5′-3′)[a]	Usage
phaC-NF	GCGTGGCGTGGATGAGATATC**GAGCTC**GACGAGTGGACGAT GTATGC	Amplify the upstream and downstream fragments of *phaC*
phaC-NR	TCATCCCTCCACGTCCATCG	gene to construct pHFX-*phaC*
phaC-CF	GACGTGGAGGGATGATCGTTTTTTCGACGTGAAAA	
phaC-CR	TATAGGGAGAAGCTT**GCATGC**CGTGAATGTACCCGAAGGTCT	
phaC1-NF	GCGTGGCGTGGATGA**GATATCGAGCTC**GGTTACTGAGAGTT TTGTCGCATCG	Amplify the upstream and downstream fragments of *phaC1* gene to construct pHFX-*phaC1*
phaC1-NR	CTTTTATCTCGAGTGTGGTGGCGAA	
phaC1-CF	CACCACACTCGAGATAAAAGTACGGCGAATCAACAGTACTAGTG AGG	
phaC1-CR	TATAGGGAGAAGCTT**GCATGC**CGCGTTTTACGAGGCACTCTC AGAAC	
phaC3-NF	GCGTGGCGTGGATGA**GATATCGAGCTC**CTTACCCAGTATGG TCCTCGACTGT	Amplify the upstream and downstream fragments of *phaC3* gene to construct pHFX-*phaC3*
phaC3-NR	GAACTATATTATCTCGAGCGAGGAT	
phaC3-CF	CGCTCGAGATAATATAGTTCCCTTAGTCCCCGTCCCGTATGAGTA	
phaC3-CR	TATAGGGAGAAGCTT**GCATGC**CGAATGCGAGAGAACCCGGTC GAGCG	
qRTphaC1-F	TCGAACGAGGTGCGGACA	qRT-PCR analysis of *phaC1* expression
qRTphaC1-R	GTCGGTTGATCAGCGCGT	
qRTphaC2-F	CGTCGGTAGCTGGCGCAC	qRT-PCR analysis of *phaC2* expression
qRTphaC2-R	TCGGGACGTTCTGCTGCA	
qRTphaC3-F	ATGGGCGTTCGAGGGTCA	qRT-PCR analysis of *phaC3* expression
qRTphaC3-R	GAGCGGCTCGTAGCGGAG	
7SF	CCAACGTAGAAACCTCGTC	Quantification of 7S rRNA
7SR	GATGGTCCGCTGCTCGCTTC	
phaC1-Pro-F	AGGTTCCACATCGTAATCTCG	Amplify the double-stranded DNA fragment of *phaC1* promoter for EMSA analysis
phaC1-Pro-R	GTAAACGGGTTCATGGTCAT	

[a] Sequences representing restriction sites are bold

endogenous control. The fold change of gene expression was analyzed according to the method developed by Schmittgen et al. (2008). The primers used are listed in Table 2.

Measurements of cell growth and determination of residual glucose concentration

Diphenylamine colorimetric method was used to measure the growth of *H. mediterranei* mutants by using Beckman Coulter DU800 spectrophotometer (Jersey City, NJ, USA), as described previously (Hou et al. 2015). The cell growth curve was plotted by using OD_{595} per mL culture against time. The residue glucose concentration in the culture was monitored by using SBA-40C biosensor analyzer (Shandong, China).

Gas chromatography

Harvested cells of *H. mediterranei* were lyophilized overnight by using TF-FD-12S freeze dryer (Shanghai, China). About 50-mg lyophilized cells were used for methanolysis reaction in 2-mL chloroform and 2-mL methanol containing 3% (vol/vol) sulfuric acid at 100 °C for 4 h. After stratification using distilled water, the constituents in the organic phase were analyzed by GC-6820 (Agilent, USA) as previously described (Han et al. 2007). In the GC analysis, benzoic acid was used as the internal standard for quantitative calculation of 3HB and 3HV. The relative mass correction factors for 3HB and 3HV were obtained from reference material PHBV and used for the quantitative analysis of monomer compositions. PHBV content was calculated as follows: (mass of PHBV/original lyophilized cell mass) × 100%. The 3HV molar content in PHA was calculated as the ratio of 3HV mole / (3HV mole + 3HB mole) (as mol%).

Transmission electron microscopy

The *H. mediterranei* strains of ΔEPSΔ*pps*-like gene, ΔEPSΔ*pps*-like gene*ΔphaCΔphaC1*, ΔEPSΔ*pps*-like gene*ΔphaCΔphaC3*, and ΔEPSΔ*pps*-like gene*ΔphaCΔphaC1ΔphaC3* were grown in PHA

production medium for 168 h and subsequently harvested for TEM analysis. TEM sample preparation was performed as previously described (Cai et al. 2012). TEM images of PHA granules were acquired on JEM-1400 transmission electron microscope (JEOL, Japan).

Electrophoretic mobility shift assay

The double-stranded DNA fragment (176 bp) of *phaC1* promoter was amplified by PCR using the primer pair of phaC1-Pro-F/phaC1-Pro-R (Table 2). The purified PCR product as the probe for EMSA was labeled with biotin by using Chemiluminescent Biotin-Labeled Nucleic Acid Detection Kit (Beyotime, China) as the manufacturer's instruction. PPS-like protein was expressed and purified from *Haloferax volcanii* H1424 as previously described (Chen et al. 2019). The EMSA was performed using Chemiluminescent EMSA Kit (Beyotime, China) with minor modifications. Briefly, PPS-like protein (0–160 pmol) were incubated with 1 fmol DNA probe in a 20 μL reaction mixture contained 1 × EMSA buffer, 1 μg/μL poly dI-dC, 20 mM Tris-HCl (pH 8.0), 2 M NaCl at 25 °C for 30 min. Then, the reaction samples were immediately loaded on a non-denaturing 8% polyacrylamide gel with 1 μL 40% sucrose solution and 0.2 μL bromophenol blue. The electrophoresis was run in 0.5 × Tris-borate-EDTA buffer at 250 V for 25 min. Subsequently, the DNA-protein complex and free probes were transferred onto a Biodyne nylon membrane (Pall, USA) by using Trans-Blot (Bio-Rad, USA). The transfer was run in 0.5 × Tris-borate-EDTA buffer at 4 °C for 30 min at electricity of 380 mA. The membrane with probes was cross-linked using Gene Linker UV Chamber (Bio-Rad, American) at C-3 gear. The biotin-labeled probes were detected by Chemiluminescent Nucleic Acid Detection Module Kit (Thermo Fisher Scientific, USA) and photographed using Tanon 5200 Multi Chemiluminescent Imaging System (Tanon, China).

Sequence analysis

An online webserver was used for predicting DNA-binding proteins (http://crdd.osdd.net/raghava/dnabinder/index.html). The parameter of SVM (support vector machine) score greater than zero indicated that the predicted protein is a DNA-binding protein.

Statistical analysis

All data were analyzed using GraphPad Prism software and presented as mean ± standard deviation (SD) of the three independent replicates. Statistical significance between groups were performed using Student's *t* test at three significance levels (*$p < 0.05$, **$p < 0.01$, and ***$p < 0.01$).

Results

pps-like gene deletion upregulates the transcription of cryptic *phaCs*

In *H. mediterranei*, the active PHA synthase encoding genes, *phaE* and *phaC*, form a PHA gene cluster with *phaR* and *phaP* on the megaplasmid pHM300 (Fig. 1a). In addition, *phaC1* and *phaC2*/*phaC3* are located on its chromosome and the megaplasmid pHM500, respectively. Our previous work found that *phaC1*, *phaC2*, and *phaC3* were not transcribed in the wild-type *H. mediterranei* strain (Han et al. 2010). Our recent published RNA-seq data showed that the three cryptic *phaC* genes were upregulated by 5-, 2-, and 3-fold, respectively, in *H. mediterranei* ΔEPSΔ*pps*-like gene compared with ΔEPS (Chen et al. 2019). However, the number of fragments per kilobase of transcript per million mapped reads (FPKM) of *phaC1*, *phaC2*, and *phaC3* was 27, 21, and 187, respectively, which was much lower than the FPKM (1250) of *phaC* gene. In order to precisely compare the expression level of the three *phaC* genes in ΔEPSΔ*pps*-like gene and ΔEPS, we carried out qRT-PCR with the RNA samples from both exponential phase and stationary phase cultures by using the specific primers (Fig. 1a and Table 2).

The qRT-PCR results were basically consistent with the RNA-seq transcription tendency (Fig. 1 b and c). The transcription level of *phaC1* was upregulated by 3- and 22-fold at exponential and stationary phase, respectively, in ΔEPSΔ*pps*-like gene compared with ΔEPS. For *phaC2* and *phaC3*, no significant change was observed at exponential phase, whereas the expression level at stationary phase was 5-fold and 3-fold higher, respectively, in the ΔEPSΔ*pps*-like gene. Our RNA-seq found that the *pps*-like gene deletion increased the functional PHA synthase expression level in *H. mediterranei*. Overexpression of PHA synthase could influence the expression level of other PHA synthesis genes, including other *phaC*s, *phaF*, and *phaI* (Kim et al. 2006; Quelas et al. 2013). In order to exclude the effect of *phaC* overexpression on the three cryptic *phaC* genes' expression, we knockout the *phaC* gene in ΔEPS and ΔEPSΔ*pps*-like gene. The expression level of *phaC1*, *phaC2*, and *phaC3* in ΔEPSΔ*phaC* was similar to ΔEPS at two growth phases (Fig. 1 b and c). It indicated that the transcription level of the three *phaC* genes was negligible in ΔEPSΔ*phaC* as in ΔEPS. However, deletion of *pps*-like gene in ΔEPSΔ*phaC* increased the expression of *phaC1*, *phaC2*, and *phaC3* more obviously compared with deletion of *pps*-like gene in ΔEPS. The transcription level of *phaC1* was almost 10- and 34-fold higher at exponential and stationary phase in ΔEPSΔ*pps*-like geneΔ*phaC*, respectively. The expression of *phaC2* showed almost 3- and 6-fold increase at exponential and stationary phase in ΔEPSΔ*pps*-like geneΔ*phaC*, respectively. In the case of *phaC3*, its expression underwent almost 6-fold

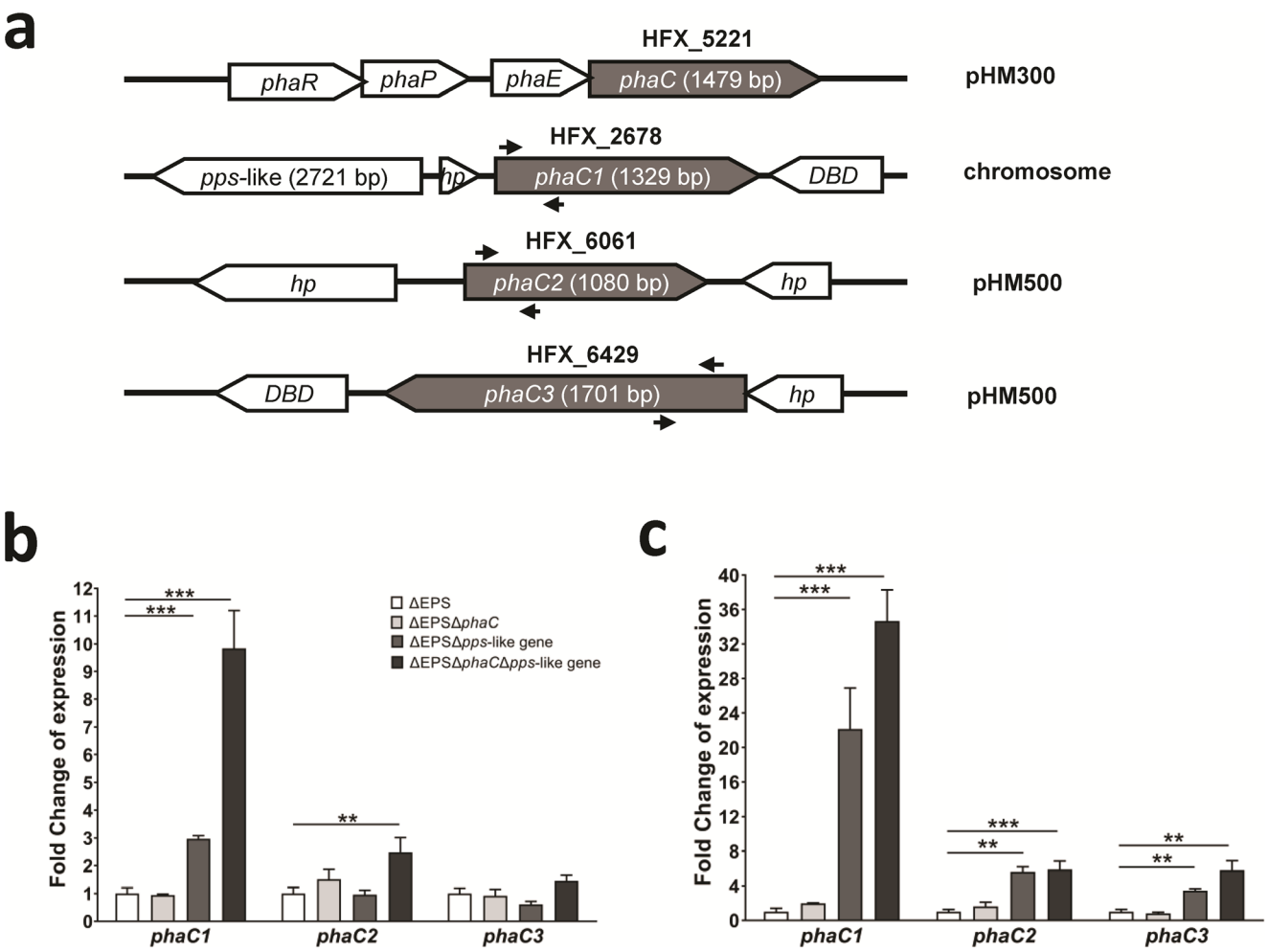

Fig. 1 Expression of three cryptic *phaC* genes in *Haloferax mediterranei* mutants. **a** Genetic organization of four *phaC* genes in *H. mediterranei*. *hp* hypothetical protein, *DBD* DNA binding domain. The location of primers used for qRT-PCR is indicated by arrows. qRT-PCR analysis of three cryptic *phaC* genes in *pps*-like gene or *phaC* gene knockouts at exponential phase (**b**) and stationary phase (**c**). All the data are represented as mean ± standard deviations from three independent experiments. $^{**}p < 0.01$, $^{***}p < 0.01$

increase at stationary phase in ΔEPSΔ*pps*-like geneΔ*phaC*. In total, deletion of the *pps*-like gene activated the expression of the cryptic *phaC* genes in *H. mediterranei*, which supported our previous findings (Chen et al. 2019). Moreover, deletion of both *phaC* and *pps*-like genes led to a more prominent upregulation of the expression level of *phaC1* than *phaC2* and *phaC3* genes. This indicated that *phaC* deletion had a positive effect on cryptic *phaC* gene expression when *pps*-like gene was deleted.

pps-like and *phaC* knockout strain accumulates PHBV

In our subsequent study, we aimed to investigate whether the expressed cryptic PhaC proteins could form a functional PHA synthase with PhaE protein in Δ*pps*-like gene strain. We tested the PHA accumulation ability of four mutant strains (ΔEPS, ΔEPSΔ*phaC*, ΔEPSΔ*pps*-like gene, ΔEPSΔ*pps*-like geneΔ*phaC*) by culturing them in PHA production media for 132 h. During the fermentation process, culture samples were taken every 12 h to measure cell growth and glucose consumption (Fig. 2a). Obviously, ΔEPSΔ*phaC* and ΔEPSΔ*pps*-like geneΔ*phaC* grew slowly compared with ΔEPS and ΔEPSΔ*pps*-like gene, respectively. Among the four tested strains, the growth rate decreased in the following order: ΔEPSΔ*pps*-like gene>ΔEPS>ΔEPSΔ*pps*-like geneΔ*phaC*>ΔEPSΔ*phaC*. The residual glucose concentration in the culture supernate showed an opposite trend with respect to the cell growth rate. These results showed that *phaC* deletion slowed down glucose consumption and simultaneously had a negative effect on cell growth in *H. mediterranei*. However, *pps*-like gene deletion increased glucose consumption and accelerated cell growth in ΔEPS and ΔEPSΔ*phaC*.

The samples at 132 h were used for PHA analysis. With the increase in the amount of intracellular PHA, the turbidity of *H. mediterranei* culture became higher. As shown in Fig. 2b, the cultures of ΔEPS and ΔEPSΔ*pps*-like gene showed greater turbidity compared with ΔEPSΔ*pps*-like geneΔ*phaC* and ΔEPSΔ*phaC*. Notably, the culture of ΔEPSΔ*phaC* was almost

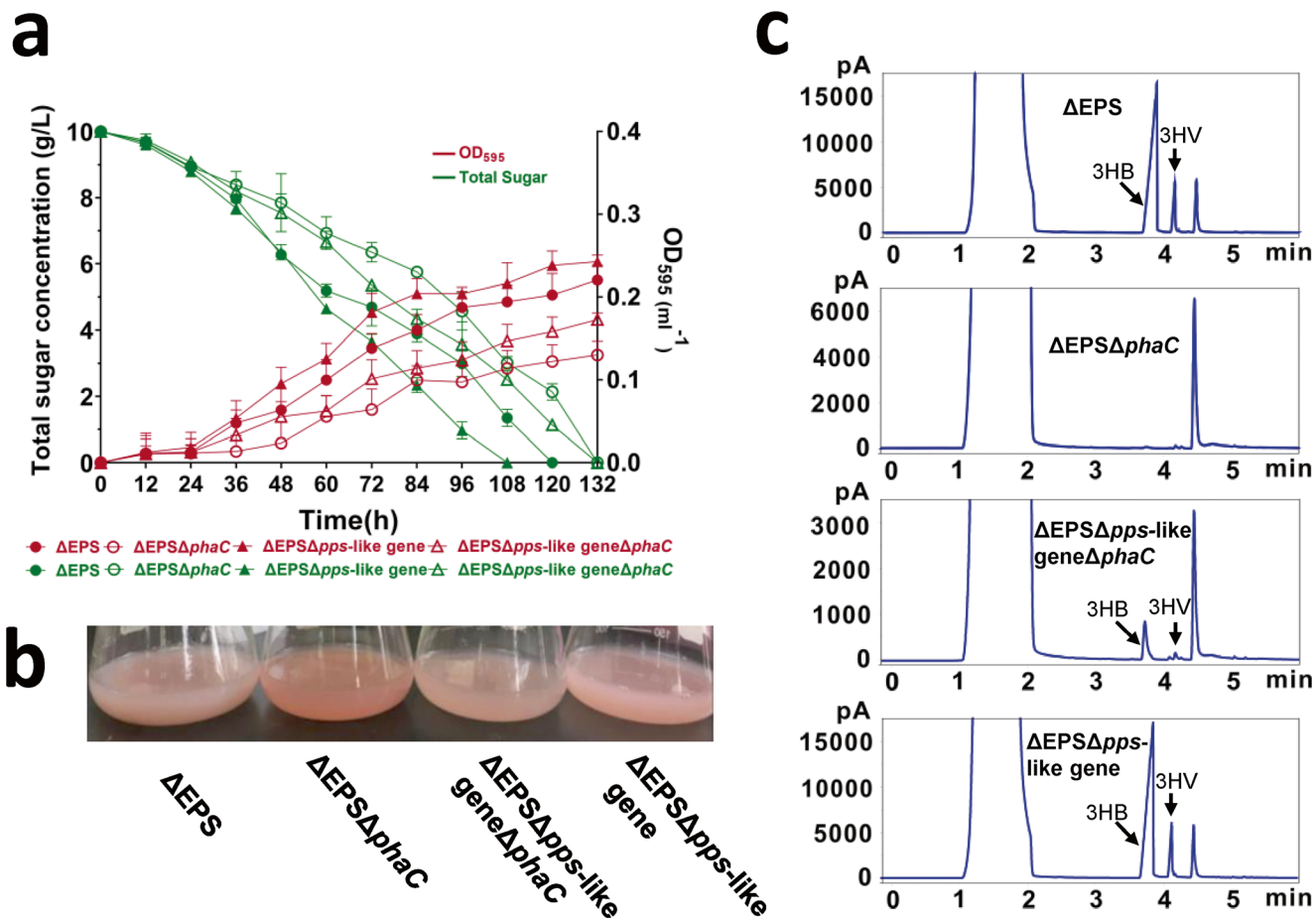

Fig. 2 Effects of *pps*-like or *phaC* knockout on cell growth, glucose consumption, and PHBV synthesis in *H. mediterranei*. **a** Time course of cell growth and glucose consumption. Green curves, glucose consumption; red curves, cell growth; closed circles, ΔEPS; open circles, ΔEPSΔ*phaC*; closed triangles, ΔEPSΔ*pps*-like gene; open triangles, ΔEPSΔ*pps*-like geneΔ*phaC*. **b** Optical images of cell cultures in PHA fermentation medium at 132 h. **c** GC analysis of PHBV accumulation in ΔEPS, ΔEPSΔ*phaC*, ΔEPSΔ*pps*-like geneΔ*phaC*, and ΔEPSΔ*pps*-like gene

transparent orange color, indicating no PHA deposited in the cells. The PHA accumulation results determined by GC analysis are shown in Table 3 and Fig. 2c. ΔEPS and ΔEPSΔ*pps*-like gene could accumulate 48% and 54% (wt) PHBV, respectively. The deletion of *phaC* in ΔEPS completely abolished its PHA accumulation ability, whereas its deletion in ΔEPSΔ*pps*-like gene still resulted in a PHBV accumulation of 5% (wt). It implied that PhaC1 and/or PhaC3 could form functional PHA synthase with the PhaE subunit and catalyzed PHBV synthesis in the *pps*-like gene deletion mutant.

Both PhaC1 and PhaC3 form functional PHA synthase with PhaE subunit in *pps*-like deletion mutant

We next wanted to know which of the three cryptic PhaCs polymerized with PhaE to accumulate PHBV in ΔEPSΔ*pps*-

Table 3 PHA accumulation in *H. mediterranei* mutant strains[a]

Strains	PHBV content (wt%)	3HV fraction (mol%)	CDW[b] (g/L)	PHBV concn (g/L)
ΔEPS	48.77 ± 0.18	10.90 ± 0.14	5.10 ± 0.08	2.49 ± 0.05
ΔEPSΔ*phaC*	0	0	2.90 ± 0.16	0
ΔEPSΔ*pps*-like gene	54.44 ± 1.24	10.55 ± 0.29	5.24 ± 0.22	2.86 ± 0.18
ΔEPSΔ*pps*-like geneΔ*phaC*	4.65 ± 1.00	35.71 ± 2.13	3.09 ± 0.20	0.14 ± 0.02

[a] Data are expressed as mean ± standard deviations from three independent experiments

[b] *CDW* cell dry weight

like gene*ΔphaC*. Thus, *phaC1*, *phaC3*, or both were further knockout in ΔEPSΔ*pps*-like gene*ΔphaC*. The parent stain (ΔEPSΔ*pps*-like gene*ΔphaC*) and obtained mutants (ΔEPSΔ*pps*-like gene*ΔphaCΔphaC1*, ΔEPSΔ*pps*-like gene*ΔphaCΔphaC3*, and ΔEPSΔ*pps*-like gene*ΔphaCΔphaC1ΔphaC3*) were then used for PHA fermentation and GC analysis. The fermentation process lasted for 228 h until the glucose in all cultures was consumed completely. The slow glucose consumption might be related to a small amount of or even no PHA synthesis (Table 4). Deletion of the *phaC1* gene reduced the PHBV content from 4 to 0.43% (wt). On the other hand, the deletion of the *phaC3* gene slightly reduced the PHBV content to 3.44% (wt). This suggested that PhaC1 had a pronounced effect on PHBV synthesis in the ΔEPSΔ*pps*-like gene*ΔphaC* strain, compared with PhaC3. However, the PHA yield in ΔEPSΔ*pps*-like gene*ΔphaCΔphaC1* and ΔEPSΔ*pps*-like gene*ΔphaCΔphaC3* mutants was very low compared with ΔEPSΔ*pps*-like gene mutant. It also implied that the expression level of *phaC1* and *phaC3* caused by *pps*-like gene deletion mutant was quite low compared with the *phaC* gene in its original strain. The knockout of both *phaC1* and *phaC3* genes in ΔEPSΔ*pps*-like gene*ΔphaC* completely abolished its PHA synthesis. Thus, PhaC2 did not participate in PHBV synthesis. The 3HV content was significantly enhanced in the *phaC1* or *phaC3* deletion mutants compared with the ΔEPSΔ*pps*-like strain. The expression of *phaC1* and *phaC3* genes resulted into the 3HV content of 48.63 and 35.11 mol%, respectively, whereas *phaC* gene expression led to a 3HV content of 10.55 mol%. This might be due to the different substrate specificities of PhaC1, PhaC3, and PhaC. The fermentation results were further verified by visualizing the PHA granules by TEM imaging (Fig. 3). Few PHA granules were observed in the strain ΔEPSΔ*pps*-like gene*ΔphaCΔphaC1*. The number of PHA granules was more and appeared bigger in size in ΔEPSΔ*pps*-like gene*ΔphaCΔphaC3*. No PHA granule was observed in ΔEPSΔ*pps*-like gene*ΔphaCΔphaC1ΔphaC3*. Despite the deletion of *phaC* gene, PhaC1 and PhaC3 formed PHA granules after the *pps*-like gene knockout. Thus, PhaC1 and PhaC3 formed an active PHA synthase complex with PhaE subunit in the Δ*pps*-like gene mutant. However, PhaC2 did not participate in PHA granule formation. This indicated that PhaC2 was incapable of forming functional PHA synthase due to its truncated C terminus. This result was consistent with our previous report that PhaC2 could not form functional PHA synthase with PhaE protein in *H. hispanica* (Han et al. 2010). Overall, in agreement with the previous two results and the fermentation results, both PhaC1 and PhaC3 could complex with PhaE subunit to form active PHA synthase and accumulate PHBV in ΔEPSΔ*pps*-like gene*ΔphaC*. Especially, PhaC1 demonstrated a significant effect on PHBV synthesis.

PPS-like protein binds to the *phaC1* promoter in vitro

The detailed mechanism behind the activation of the three cryptic *phaC* genes in *pps*-like gene deleted *H. mediterranei* remained to be clarified. PPS-like protein has no PPS enzyme activity although it shows high homology with PPS family proteins (Chen et al. 2019). Then, we tentatively speculated that PPS-like protein might regulate its target genes by binding their promoters and performed a prediction by using an online webserver (http://crdd.osdd.net/raghava/dnabinder/index.html). The SVM score of PPS-like protein is 0.89 and thus probably possessed DNA sequence binding ability. We chose *phaC1* gene as the target gene to test the DNA-binding capability of PPS-like protein due to the follow reasons. Our qRT-PCR and fermentation results revealed that among the three cryptic *phaC* genes, *phaC1* was upregulated most prominently and played the most important role in PHA polymerization in *pps*-like gene and *phaC* gene deletion mutants. In addition, *phaC1* and *pps*-like gene are closely linked and separated by only one small gene with unknown function on the chromosome (Fig. 1a). This indicated that the interaction between PPS-like and the promoter sequence of *phaC1* has a high probability. The 176 bp promoter sequence of *phaC1* embracing its core elements, BRE and TATA box, was amplified (Fig. 4a and Table 2) to test whether the *phaC1*

Table 4 PHA accumulation in *H. mediterranei* mutant strains[a]

Strains	PHBV content (wt%)	3HV fraction (mol%)	CDW[b] (g/L)	PHBV concn (g/L)
ΔEPSΔ*pps*-like gene*ΔphaC*	3.75 ± 1.15	33.33 ± 2.13	3.21 ± 0.48	0.12 ± 0.01
ΔEPSΔ*pps*-like gene*ΔphaCΔphaC1*	0.43 ± 0.15	35.11 ± 1.72	2.32 ± 0.51	0.01 ± 0.001
ΔEPSΔ*pps*-like gene*ΔphaCΔphaC3*	3.44 ± 0.71	48.63 ± 3.25	2.89 ± 0.35	0.10 ± 0.01
ΔEPSΔ*pps*-like gene*ΔphaCΔpha*C1Δ*phaC3*	0	0	2.91 ± 1.23	0

[a] Data are expressed as mean ± standard deviations from three independent experiments

[b] *CDW* cell dry weight

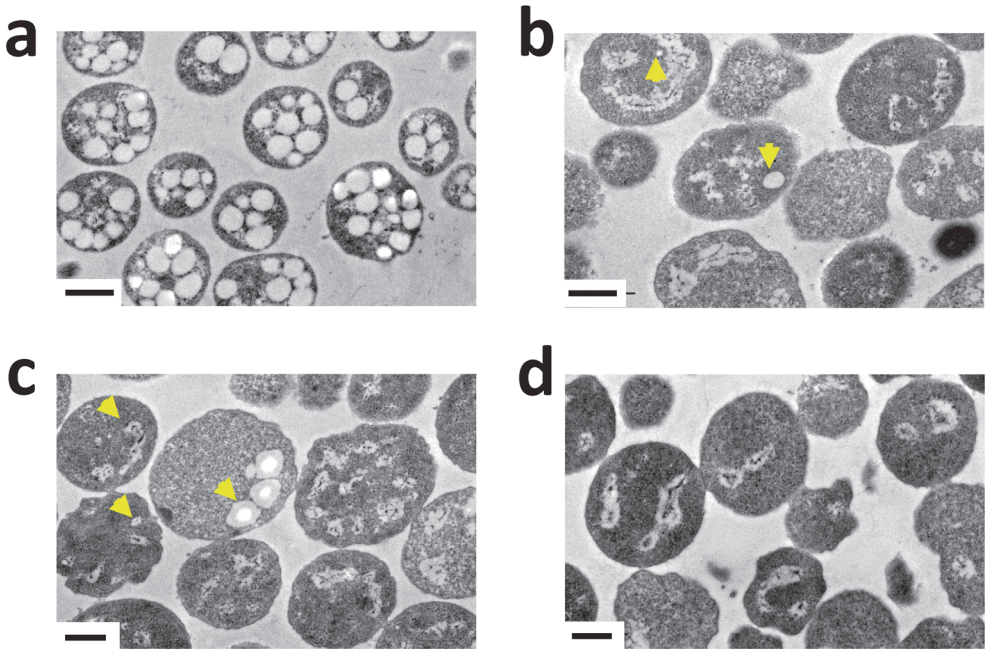

Fig. 3 TEM images of *pps*-like *and phaCs* deletion *H. mediterranei* mutants grown in PHA fermentation medium for 168 h. **a** ΔEPSΔ*pps*-like gene; **b** ΔEPSΔ*pps*-like geneΔ*phaC*Δ*phaC1*; **c** ΔEPSΔ*pps*-like geneΔ*phaC*Δ*phaC1*Δ*phaC3*; **d** ΔEPSΔ*pps*-like geneΔ*phaC*Δ*phaC3*. PHA granules observed in (**b**) and (**c**) are indicated by yellow arrows. Scar bars are 0.5 μm

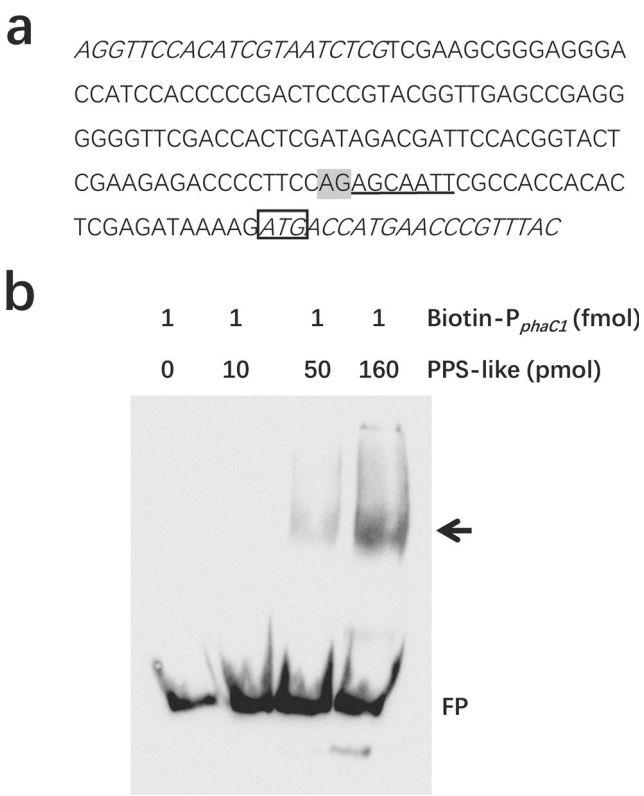

Fig. 4 EMSA analysis of the interaction between PPS-like protein and the double-stranded DNA fragment of *phaC1* promoter. **a** Nucleotide sequences of *phaC1* promoter used for EMSA. The length of the DNA probe was 176 bp. The predicted BRE and TATA box were shaded and double underlined, respectively. The start code of *phaC1* was boxed. The primers for PCR were in italic. **b** EMSA of PPS-like protein and *phaC1* promoter. The amount of DNA probe (1 fmol) and proteins (0–160 pmol) in each lane was indicated. The DNA protein complex was indicated by arrows. *FP* free probes

promoter could be recognized by PPS-like protein overexpressed and purified from *Haloferax volcanii*. Their interaction was determined by electrophoretic mobility shift assay (EMSA) (Fig. 4b). As we predicted, PPS-like protein could efficiently bind to the *phaC1* promoter sequence deduced from a clear binding band observed by EMSA analysis (Fig. 4b). At a fixed DNA concentration of 1 fmol, the increasing concentration of PPS-like protein resulted in the formation of more protein-DNA complex. PPS-like could bind to *phaC1* promoter sequence at the protein concentration of 50 pmol. As the protein concentration increased to 160 pmol, the formed PPS-like DNA complex was significantly intensified (Fig. 4b). This result might help explain the upregulation of *phaC1* gene expression after *pps*-like gene deletion, as PPS-like protein repressed *phaC1* expression by binding to its promoter sequence.

Discussion

The present study showed that the deletion of *pps*-like gene in *H. mediterranei* activated the expression of three cryptic *phaC* genes, especially *phaC1*, although their absolute transcription was low. PPS-like protein probably negatively regulated the expression level of *phaC1* by binding to its promoter region. It was also found that PhaC1 and PhaC3 could form functional PHA synthases with PhaE and accumulated PHBV in ΔEPSΔ*pps*-like geneΔ*phaC*. However, the expression of *phaC2* alone completely abolished the PHBV synthesis capability. The 3HV content in the PHBV synthesized by the *phaC* mutants were significantly higher compared with the

ΔEPSΔ*pps*-like strain. PhaC1 contributed to the highest 3HV mol%, followed by PhaC3 and finally PhaC.

H. mediterranei wild-type strain has four *phaC* encoding genes. Only the *phaC* gene in the *pha* cluster is expressed, and the other three *phaC* genes are cryptic under PHA-accumulating condition. The presence of multiple PHA synthase genes is a common phenomenon among PHA-accumulating microorganisms. For example, *Pseudomonas* species usually possess at least two PHA synthase encoding genes. *Pseudomonas mendocina* genome encoded two PHA synthase genes (Hein et al. 2002). Both the PHA synthase genes were functional and conferred PHA synthesis when expressed individually in PHA-negative mutants. However, PhaC1 was the major PHA synthase and accumulated higher PHA content with fatty acid as a sole carbon source, while PhaC2 accumulated a higher concentration of PHA using gluconate under storage conditions. *Pseudomonas oleovorans* and *Pseudomonas putida* strains were reported to contain even more than two PHA synthase genes that influenced the PHA monomer composition (Matsusaki et al. 1998). *Ralstonia eutropha* has two PHA synthase encoding genes, *phaC1* and *phaC2* (Peplinski et al. 2010). *phaC1* gene was constitutively expressed and encoded the major PHA synthase enzyme. *phaC2* was not transcribed under all conditions except during storage conditions using gluconate as sole carbon source. Moreover, deletion of *phaC1* gene inactivated *phaC2* gene. The PHA gene locus in *Burkholderia* sp. included two PHA synthase genes, each of them encoding functional enzyme, probably with distinct substrate specificity (de Andrade Rodrigues et al. 2000; Hang et al. 2002). The genome of *Neptunomonas concharum* JCM17730 contained two class I PHA synthases, PhaC1 and PhaC2, and one class III PHA synthase, PhaEC (Pu et al. 2020). Heterologous expression of the individual PHA synthase genes in *E. coli* showed that the three *phaC* genes exhibited different catalytic activities at different cultivation temperatures (Pu et al. 2020). PhaC1 presented the highest PHA synthesis ability, followed by PhaEC and PhaC2. Several *Halomonas* species have been reported to encode two different *phaC* genes. The two PhaC proteins from *Halomonas* sp. TD01 showed 78% and 73% identity with the two PhaCs from *Halomonas elongata* DSM2581, respectively (Cai et al. 2011). The heterologous expression of $phaC1_{He}$ from *H. elongate* DSM 2581 accumulated PHA in *E. coli* (Ilham et al. 2014). However, $phaC2_{He}$ expression in *E. coli* did not synthesize PHA. Furthermore, coexpression of *phaC1* and *phaC2* genes from *Halomonas* sp. O-1 resulted in an effect similar to *phaC1* expression alone in *E. coli* (Ilham et al. 2014). This indicated that *Halomonas phaC2* was non-functional. A total of 5 *phaC* genes were annotated in the genome of *Bradyrhizobium japonicus* UDSA 110 (Quelas et al. 2013).

It has been observed that PHA synthase gene expression influenced the expression level of other PHA biosynthesis genes, positively or negatively. For instance, *phaC2* overexpression in *P. putida* elevated the transcription level of its two PHA granule-associated genes, *phaF* and *phaI* (Kim et al. 2006). *B. japonicum* USDA 110 genome had five paralogs of PHA synthase genes belonging to different classes (Quelas et al. 2013). PhaC1 was similar to rhizobial PHA synthase and belonged to class I type. PhaC2 was unclassified and related to PHA synthase from betaproteobacteria. PhaC3, PhaC4, and PhaC5 belonged to class I, class III, and class IV, respectively. Among them, *phaC1* and *phaC2* were significantly expressed, but *phaC3*, *phaC4*, and *phaC5* expression level was very low. *phaC1* was the main PHA synthase as its deletion mutant could not synthesize PHA. Interestingly, Δ*phaC2* mutant increased *phaC3* transcript and synthesized more PHA than wild type, suggesting that *phaC2* negatively regulated PHA synthesis. Similarly, in the case of *Rhodospirillum rubrum* possessing three *phaC* genes, PhaC2 was the major PHA synthase. However, deletion of *phaC1* gene elevated the PHA production level, indicating that PhaC1 exerted inhibitory effect on PHA synthesis (Jin and Nikolau 2012). In this study performed in *H. mediterranei*, prior to the deletion of the cryptic genes in ΔEPSΔ*pps*-like gene mutant, *phaC* gene was knockout. This strategy helped to determine the sole effect of the cryptic genes on PHBV synthesis upon *pps*-like gene deletion. Our results showed that besides the regulation of *phaC1* imposed by PPS-like protein, it was probable that overexpression of *phaEC* gene caused by the deletion of *pps*-like gene in *H. mediterranei* had influenced the expression of *phaC1*, *phaC2*, and *phaC3* genes (Fig. 1 b and c). Moreover, the fact that the three PhaC proteins, PhaC, PhaC1, and PhaC3 led to incorporation of different molar fractions of 3HV showed their distinct substrate specificity. Thus, engineering of these genes can possibly produce different PHBV materials with tailor-made 3HV content.

The expression of *phaC* is often regulated by DNA binding regulatory proteins. In *P. oleovorans*, PhaF negatively regulated the expression of *phaC1* by binding to the promoter of *phaC1* (Prieto et al. 1999). Additionally, *Pseudomonas* sp. encodes a PhaD protein which is a TetR-like transcriptional regulator. PhaD could bind the promoter of *phaC1*, which directed the transcription of *phaC1ZC2D* operon (de Eugenio et al. 2010). In *B. japonicum* USDA 110, expression of *phaC5* and *phaC3* was elevated when *phaR* gene, encoding a DNA binding PHA granule associated protein, was deleted (Nishihata et al. 2018). In *Azotobacter vinelandii*, PhbR protein is a transcriptional activator of *phbBAC* operon (Peralta-Gil et al. 2002). However, in the case of PPS-like mediated regulation, we had two important findings. First, *pps*-like gene knockout led to upregulated *phaEC* expression and enhanced PHA accumulation with no disorder in granule formation. Second, PPS-like protein repressed *phaC1* expression by binding to its promoter region, and hence its deletion

upregulated *phaC1* gene expression. This type of regulation phenomenon by PPS-like protein is identified in PHA accumulating microorganisms for the first time. However, the specific binding sites of *phaC1* promoter by PPS-like protein need to be further determined in our future study.

PPS belongs to the PEP-utilizing family of protein. The function of PPS is quite diverse among various microorganisms. It is normally involved in the gluconeogenic direction of carbohydrate metabolism and catalyzes the conversion of pyruvate to PEP (Niersbach et al. 1992). However, there are reports that PPS has a bidirectional activity and participates in the glycolytic direction, i.e., conversion of PEP to pyruvate in microorganisms like *Pyrococcus furiosus* (Sakuraba et al. 2001). In *Thermococcus kodakarensis*, PPS enzyme played a vital role in the conversion of PEP to pyruvate as the strain failed to grow on maltooligosaccharides upon the deletion of *pps* gene (Imanaka et al. 2006). Pyruvate phosphate dikinase (PPDK) has a similar structure and function with PPS and also belongs to PEP-utilizing family. In thermophilic archaeon *Thermoproteus tenax*, PPDK showed a bidirectional activity in PEP/pyruvate interconversion with preference for PEP conversion to pyruvate (Tjaden et al. 2006). In *Microbispora rosea*, PPDK is involved in the gluconeogenic pathway, catalyzing the formation of PEP from pyruvate (Eisaki et al. 1999). PPDK is an important rate-limiting enzyme in C4 photosynthetic pathway in plants. It is involved in diverse processes in plants, including abiotic stress tolerance, early seedling growth, seed development, conversion of NADH to NADPH, maintenance of pH and replenishing citric acid cycle intermediates for amino acid synthesis, nitrogen assimilation and fatty acid synthesis (Yadav et al. 2020). A very close structural homolog to PPS and PPDK protein is rifampin phosphotransferases (RPH). It is an antibiotic resistance protein, widespread among pathogenic bacteria that confer resistance to rifamycin by phosphorylation (Qi et al. 2016). Similarly, multiple sequence alignment and phylogenetic tree analysis showed that PPS-like protein was closely related to both PPS and PPDK proteins (Chen et al. 2019). However, it neither possessed PPS nor PPDK function. Rather, our present study revealed its regulatory function on *phaC1* gene. Thus, even though all these proteins showed high homology, they have evolved diverse functions. Taken together, molecular characterization of PPS-like protein and its involvement in PHBV synthesis enhancement has provided a new insight on both the PHA biosynthesis in haloarchaea and the diversity of PPS family protein functions.

Acknowledgments The authors thank Jingnan Liang (Public Technology Service Center of Institute of Microbiology, CAS) in TEM observation.

Authors' contributions JH, HX, and JC designed the experiments. JC performed the experiments. JC and RM analyzed the data. JH, RM, and HX wrote the manuscript. All of the authors read and approved the final version of the manuscript.

Funding This work was financially supported by grants from funding from National Key R&D Program of China (No. 2020YFA0906800), and the National Natural Science Foundation of China (No. 31970031 and No. 91751201).

Compliance with ethical standards

This article does not contain any studies with human participants or animals performed by any of the authors.

Conflict of interest The authors declare that they have no conflict of interest.

References

Alsafadi D, Al-Mashaqbeh O (2017) A one-stage cultivation process for the production of poly-3-(hydroxybutyrate-*co*-hydroxyvalerate) from olive mill wastewater by *Haloferax mediterranei*. New Biotechnol 34:47–53. https://doi.org/10.1016/j.nbt.2016.05.003

Bhattacharyya A, Pramanik A, Maji SK, Haldar S, Mukhopadhyay UK, Mukherjee J (2012) Utilization of vinasse for production of poly-3-(hydroxybutyrate-*co*-hydroxyvalerate) by *Haloferax mediterranei*. AMB Express 2(1):34. https://doi.org/10.1186/2191-0855-2-34

Bhattacharyya A, Saha J, Haldar S, Bhowmic A, Mukhopadhyay UK, Mukherjee J (2014) Production of poly-3-(hydroxybutyrate-*co*-hydroxyvalerate) by *Haloferax mediterranei* using rice-based ethanol stillage with simultaneous recovery and re-use of medium salts. Extremophiles 18(2):463–470. https://doi.org/10.1007/s11274-015-1823-4

Bhattacharyya A, Jana K, Haldar S, Bhowmic A, Mukhopadhyay UK, De S, Mukherjee J (2015) Integration of poly-3-(hydroxybutyrate-*co*-hydroxyvalerate) production by *Haloferax mediterranei* through utilization of stillage from rice-based ethanol manufacture in India and its techno-economic analysis. World J Microbiol Biotechnol 31(5): 717–727. https://doi.org/10.1007/s11274-015-1823-4

Cai L, Tan D, Aibaidula G, Dong XR, Chen JC, Tian WD, Chen GQ (2011) Comparative genomics study of polyhydroxyalkanoates (PHA) and ectoine relevant genes from *Halomonas* sp. TD01 revealed extensive horizontal gene transfer events and co-evolutionary relationships. Microb Cell Factories 10:88. https://doi.org/10.1186/1475-2859-10-88

Cai S, Cai L, Liu H, Liu X, Han J, Zhou J, Xiang H (2012) Identification of the haloarchaeal phasin (PhaP) that functions in polyhydroxyalkanoate accumulation and granule formation in *Haloferax mediterranei*. Appl Environ Microbiol 78(6):1946–1952. https://doi.org/10.1128/AEM.07114-11

Cai S, Cai L, Zhao D, Liu G, Han J, Zhou J, Xiang H (2015) A novel DNA-binding protein, PhaR, plays a central role in the regulation of polyhydroxyalkanoate accumulation and granule formation in the haloarchaeon *Haloferax mediterranei*. Appl Environ Microbiol 81(1):373–385. https://doi.org/10.1128/AEM.02878-14

Chen J, Mitra R, Zhang S, Zuo Z, Lin L, Zhao D, Xiang H, Han J (2019) Unusual phosphoenolpyruvate (PEP) synthetase-like protein crucial to enhancement of polyhydroxyalkanoate accumulation in *Haloferax mediterranei* revealed by dissection of PEP-pyruvate interconversion mechanism. Appl Environ Microbiol 85(19). https://doi.org/10.1128/AEM.00984-19

Cline SW, Lam WL, Charlebois RL, Schalkwyk LC, Doolittle WF (1989) Transformation methods for halophilic archaebacteria. Can J Microbiol 35(1):148–152. https://doi.org/10.1139/m89-022

de Andrade Rodrigues MF, Vicente EJ, Steinbuchel A (2000) Studies on polyhydroxyalkanoate (PHA) accumulation in a PHA synthase I-negative mutant of *Burkholderia cepacia* generated by

homogenotization. FEMS Microbiol Lett 193(1):179–185. https://doi.org/10.1111/j.1574-6968.2000.tb09421.x

de Eugenio LI, Galan B, Escapa IF, Maestro B, Sanz JM, Garcia JL, Prieto MA (2010) The PhaD regulator controls the simultaneous expression of the pha genes involved in polyhydroxyalkanoate metabolism and turnover in *Pseudomonas putida* KT2442. Environ Microbiol 12(6):1591–1603. https://doi.org/10.1111/j.1462-2920.2010.02199.x

Eisaki N, Tatsumi H, Murakami S, Horiuchi T (1999) Pyruvate phosphate dikinase from a thermophilic actinomyces *Microbispora rosea* subsp. aerata: purification, characterization and molecular cloning of the gene. Biochim Biophys Acta 1431(2):363–373. https://doi.org/10.1016/s0167-4838(99)00057-6

Fendrihan S, Legat A, Pfaffenhuemer M, Gruber C, Weidler G, Gerbl F, Stan-Lotter H (2006) Extremely halophilic archaea and the issue of long-term microbial survival. Rev Environ Sci Biotechnol 5(2–3):203–218. https://doi.org/10.1007/s11157-006-0007-y

Han J, Lu Q, Zhou L, Zhou J, Xiang H (2007) Molecular characterization of the $phaEC_{Hm}$ genes, required for biosynthesis of poly(3-hydroxybutyrate) in the extremely halophilic archaeon *Haloarcula marismortui*. Appl Environ Microbiol 73(19):6058–6065. https://doi.org/10.1128/AEM.00953-07

Han J, Li M, Hou J, Wu L, Zhou J, Xiang H (2010) Comparison of four *phaC* genes from *Haloferax mediterranei* and their function in different PHBV copolymer biosyntheses in *Haloarcula hispanica*. Saline Syst 6:9. https://doi.org/10.1186/1746-1448-6-9

Han J, Zhang F, Hou J, Liu XQ, Li M, Liu HL, Cai L, Zhang B, Chen YP, Zhou J, Hu SN, Xiang H (2012) Complete genome sequence of the metabolically versatile halophilic archaeon *Haloferax mediterranei*, a poly(3-hydroxybutyrate-*co*-3-hydroxyvalerate) producer. J Bacteriol 194(16):4463–4464. https://doi.org/10.1128/JB.00880-12

Han J, Hou J, Zhang F, Ai G, Li M, Cai S, Liu H, Wang L, Wang Z, Zhang S, Cai L, Zhao D, Zhou J, Xiang H (2013) Multiple propionyl coenzyme A-supplying pathways for production of the bioplastic poly(3-hydroxybutyrate-*co*-3-hydroxyvalerate) in *Haloferax mediterranei*. Appl Environ Microbiol 79(9):2922–2931. https://doi.org/10.1128/AEM.03915-12

Han J, Wu LP, Hou J, Zhao DH, Xiang H (2015) Biosynthesis, characterization, and hemostasis potential of tailor-made poly(3-hydroxybutyrate-*co*-3-hydroxyvalerate) produced by *Haloferax mediterranei*. Biomacromolecules 16(2):578–588. https://doi.org/10.1021/bm5016267

Han J, Wu LP, Liu XB, Hou J, Zhao LL, Chen JY, Zhao DH, Xiang H (2017) Biodegradation and biocompatibility of haloarchaea-produced poly(3-hydroxybutyrate-*co*-3-hydroxyvalerate) copolymers. Biomaterials 139:172–186. https://doi.org/10.1016/j.biomaterials.2017.06.006

Hang X, Zhang G, Wang G, Zhao X, Chen GQ (2002) PCR cloning of polyhydroxyalkanoate biosynthesis genes from *Burkholderia caryophylli* and their functional expression in recombinant *Escherichia coli*. FEMS Microbiol Lett 210(1):49–54. https://doi.org/10.1111/j.1574-6968.2002.tb11158.x

Hein S, Paletta JR, Steinbuchel A (2002) Cloning, characterization and comparison of the *Pseudomonas mendocina* polyhydroxyalkanoate synthases PhaC1 and PhaC2. Appl Microbiol Biotechnol 58(2):229–236. https://doi.org/10.1007/s00253-001-0863-x

Hezayen FF, Steinbüchel A, Rehm BHA (2002) Biochemical and enzymological properties of the polyhydroxybutyrate synthase from the extremely halophilic archaeon strain 56. Arch Biochem Biophys 403(2):284–291. https://doi.org/10.1016/S0003-9861(02)00234-5

Hong SG, Hsu HW, Ye MT (2013) Thermal properties and applications of low molecular weight polyhydroxybutyrate. J Therm Anal Calorim 111(2):1243–1250. https://doi.org/10.1007/s10973-012-2503-3

Hou J, Feng B, Han J, Liu H, Zhao D, Zhou J, Xiang H (2013) Haloarchaeal-type beta-ketothiolases involved in poly(3-hydroxybutyrate-*co*-3-hydroxyvalerate) synthesis in *Haloferax mediterranei*. Appl Environ Microbiol 79(17):5104–5111. https://doi.org/10.1128/AEM.01370-13

Hou J, Han J, Cai L, Zhou J, Lu Y, Jin C, Liu JF, Xiang H (2014) Characterization of genes for chitin catabolism in *Haloferax mediterranei*. Appl Microbiol Biotechnol 98(3):1185–1194. https://doi.org/10.1007/s00253-013-4969-8

Hou J, Xiang H, Han J (2015) Propionyl coenzyme A (propionyl-CoA) carboxylase in *Haloferax mediterranei*: indispensability for propionyl-CoA assimilation and impacts on global metabolism. Appl Environ Microbiol 81(2):794–804. https://doi.org/10.1128/AEM.03167-14

Ilham M, Nakanomori S, Kihara T, Hokamura A, Matsusaki H, Tsuge T, Mizuno K (2014) Characterization of polyhydroxyalkanoate synthases from *Halomonas* sp. O-1 and *Halomonas elongata* DSM2581: site-directed mutagenesis and recombinant expression. Polym Degrad Stab 109:416–423. https://doi.org/10.1016/j.polymdegradstab.2014.04.024

Imanaka H, Yamatsu A, Fukui T, Atomi H, Imanaka T (2006) Phosphoenolpyruvate synthase plays an essential role for glycolysis in the modified Embden-Meyerhof pathway in *Thermococcus kodakarensis*. Mol Microbiol 61(4):898–909. https://doi.org/10.1111/j.1365-2958.2006.05287.x

Jin HN, Nikolau BJ (2012) Role of genetic redundancy in polyhydroxyalkanoate (PHA) polymerases in PHA biosynthesis in *Rhodospirillum rubrum*. J Bacteriol 194(20):5522–5529. https://doi.org/10.1128/JB.01111-12

Kim TK, Jung YM, Vo MT, Shioya S, Lee YH (2006) Metabolic engineering and characterization of *phaC1* and *phaC2* genes from *Pseudomonas putida* KCTC1639 for overproduction of medium-chain-length polyhydroxyalkanoate. Biotechnol Prog 22(6):1541–1546. https://doi.org/10.1021/bp0601746

Legat A, Gruber C, Zangger K, Wanner G, Stan-Lotter H (2010) Identification of polyhydroxyalkanoates in *Halococcus* and other haloarchaeal species. Appl Microbiol Biotechnol 87(3):1119–1127

Liu H, Han J, Liu X, Zhou J, Xiang H (2011) Development of *pyrF*-based gene knockout systems for genome-wide manipulation of the archaea *Haloferax mediterranei* and *Haloarcula hispanica*. J Genet Genomics 38(6):261–269. https://doi.org/10.1016/j.jgg.2011.05.003

Liu G, Hou J, Cai S, Zhao D, Cai L, Han J, Zhou J, Xiang H (2015) A patatin-like protein associated with the polyhydroxyalkanoate (PHA) granules of *Haloferax mediterranei* acts as an efficient depolymerase in the degradation of native PHA. Appl Environ Microbiol 81(9):3029–3038. https://doi.org/10.1128/AEM.04269-14

Liu GM, Cai SF, Hou J, Zhao DH, Han J, Zhou J, Xiang H (2016) Enoyl-CoA hydratase mediates polyhydroxyalkanoate mobilization in *Haloferax mediterranei*. Sci Rep-Uk 6:24015. https://doi.org/10.1038/srep24015

Lu QH, Han J, Zhou LG, Zhou J, Xiang H (2008) Genetic and biochemical characterization of the poly(3-hydroxybutyrate-*co*-3-hydroxyvalerate) synthase in *Haloferax mediterranei*. J Bacteriol 190(12):4173–4180. https://doi.org/10.1128/JB.00134-08

Matsusaki H, Manji S, Taguchi K, Kato M, Fukui T, Doi Y (1998) Cloning and molecular analysis of the poly(3-hydroxybutyrate) and poly(3-hydroxybutyrate-*co*-3-hydroxyalkanoate) biosynthesis genes in *Pseudomonas* sp. strain 61-3. J Bacteriol 180(24):6459–6467. https://doi.org/10.1128/JB.180.24.6459-6467.1998

Mitra R, Xu T, Xiang H, Han J (2020) Current developments on polyhydroxyalkanoates synthesis by using halophiles as a promising cell factory. Microb Cell Factories 19(1):86. https://doi.org/10.1186/s12934-020-01342-z

Niersbach M, Kreuzaler F, Geerse RH, Postma PW, Hirsch HJ (1992) Cloning and nucleotide sequence of the *Escherichia coli* K-12 *ppsA*

gene, encoding PEP synthase. Mol Gen Genet 231(2):332–336. https://doi.org/10.1007/BF00279808

Nishihata S, Kondo T, Tanaka K, Ishikawa S, Takenaka S, Kang CM, Yoshida K (2018) *Bradyrhizobium diazoefficiens* USDA110 PhaR functions for pleiotropic regulation of cellular processes besides PHB accumulation. BMC Microbiol 18(1):156. https://doi.org/10.1186/s12866-018-1317-2

Orellana R, Macaya C, Bravo G, Dorochesi F, Cumsille A, Valencia R, Rojas C, Seeger M (2018) Living at the frontiers of life: extremophiles in Chile and their potential for bioremediation. Front Microbiol 9:2309. https://doi.org/10.3389/fmicb.2018.02309

Pais J, Serafim LS, Freitas F, Reis MAM (2016) Conversion of cheese whey into poly(3-hydroxybutyrate-*co*-3-hydroxyvalerate) by *Haloferax mediterranei*. New Biotechnol 33(1):224–230. https://doi.org/10.1016/j.nbt.2015.06.001

Peplinski K, Ehrenreich A, Doring C, Bomeke M, Reinecke F, Hutmacher C, Steinbuchel A (2010) Genome-wide transcriptome analyses of the 'Knallgas' bacterium *Ralstonia eutropha* H16 with regard to polyhydroxyalkanoate metabolism. Microbiology 156:2136–2152. https://doi.org/10.1099/mic.0.038380-0

Peralta-Gil M, Segura D, Guzman J, Servin-Gonzalez L, Espin G (2002) Expression of the *Azotobacter vinelandii* poly-beta-hydroxybutyrate biosynthetic *phbBAC* operon is driven by two overlapping promoters and is dependent on the transcriptional activator PhbR. J Bacteriol 184(20):5672–5677. https://doi.org/10.1128/jb.184.20.5672-5677.2002

Prieto MA, Buhler B, Jung K, Witholt B, Kessler B (1999) PhaF, a polyhydroxyalkanoate-granule-associated protein of *Pseudomonas oleovorans* GPo1 involved in the regulatory expression system for *pha* genes. J Bacteriol 181(3):858–868. https://doi.org/10.1128/JB.181.3.858-868.1999

Pu N, Wang MR, Li ZJ (2020) Characterization of polyhydroxyalkanoate synthases from the marine bacterium *Neptunomonas concharum* JCM17730. J Biotechnol 319:69–73. https://doi.org/10.1016/j.jbiotec.2020.06.002

Qi X, Lin W, Ma M, Wang C, He Y, He N, Gao J, Zhou H, Xiao Y, Wang Y, Zhang P (2016) Structural basis of rifampin inactivation by rifampin phosphotransferase. Proc Natl Acad Sci U S A 113(14):3803–3808. https://doi.org/10.1073/pnas.1523614113

Quelas JI, Mongiardini EJ, Perez-Gimenez J, Parisi G, Lodeiro AR (2013) Analysis of two polyhydroxyalkanoate synthases in *Bradyrhizobium japonicum* USDA 110. J Bacteriol 195(14):3145–3155. https://doi.org/10.1128/JB.02203-12

Sakuraba H, Utsumi E, Schreier HJ, Ohshima T (2001) Transcriptional regulation of phosphoenolpyruvate synthase by maltose in the hyperthermophilic archaeon, *Pyrococcus furiosus*. J Biosci Bioeng 92(2):108–113. https://doi.org/10.1263/jbb.92.108

Sambrook J, Fritsch EF, Maniatis T (1989) Molecular cloning: a laboratory manual, 2nd edn. Cold Spring Harbor Laboratory Press, Cold Spring Harbor

Schmittgen TD, Livak KJ (2008) Analyzing real-time PCR data by the comparative C(T) method. Nat Protoc 3(6):1101–1108. https://doi.org/10.1038/nprot.2008.73

Shih CJ, Chen SC, Weng CY, Lai MC, Yang YL (2015) Rapid identification of haloarchaea and methanoarchaea using the matrix assisted laser desorption/ionization time-of-flight mass spectrometry. Sci Rep-UK 5:16326. https://doi.org/10.1038/srep16326

Siroosi M, Amoozegar MA, Khajeh K, Fazeli M, Rezaei MH (2014) Purification and characterization of a novel extracellular halophilic and organic solvent-tolerant amylopullulanase from the haloarchaeon, *Halorubrum* sp. strain Ha25. Extremophiles 18(1):25–33. https://doi.org/10.1007/s00792-013-0589-6

Tjaden B, Plagens A, Dorr C, Siebers B, Hensel R (2006) Phosphoenolpyruvate synthetase and pyruvate, phosphate dikinase of *Thermoproteus tenax*: key pieces in the puzzle of archaeal carbohydrate metabolism. Mol Microbiol 60(2):287–298. https://doi.org/10.1111/j.1365-2958.2006.05098.x

Xue Q, Liu XB, Lao YH, Wu LP, Wang D, Zuo ZQ, Chen JY, Hou J, Bei YY, Wu XF, Leong KW, Xiang H, Han J (2018) Anti-infective biomaterials with surface-decorated tachyplesin I. Biomaterials 178:351–362. https://doi.org/10.1016/j.biomaterials.2018.05.008

Yadav S, Rathore MS, Mishra A (2020) The pyruvate-phosphate dikinase (C4-SmPPDK) gene from *Suaeda monoica* enhances photosynthesis, carbon assimilation, and abiotic stress tolerance in a C3 plant under elevated CO_2 conditions. Front Plant Sci 11:345. https://doi.org/10.3389/fpls.2020.00345

Zhao D, Cai L, Wu J, Li M, Liu H, Han J, Zhou J, Xiang H (2013) Improving polyhydroxyalkanoate production by knocking out the genes involved in exopolysaccharide biosynthesis in *Haloferax mediterranei*. Appl Microbiol Biotechnol 97(7):3027–3036. https://doi.org/10.1007/s00253-012-4415-3

Zhao Y-X, Rao Z-M, Xue Y-F, Gong P, Ji Y-Z, Ma Y-H (2015) Poly(3-hydroxybutyrate-*co*-3-hydroxyvalerate) production by Haloarchaeon *Halogranum amylolyticum*. Appl Microbiol Biotechnol 99(18):7639–7649. https://doi.org/10.1007/s00253-015-6609-y

Zuo ZQ, Xue Q, Zhou J, Zhao DH, Han J, Xiang H (2018) Engineering *Haloferax mediterranei* as an efficient platform for high level production of lycopene. Front Microbiol 9:2893. https://doi.org/10.3389/fmicb.2018.02893